Controlling polarization twisting of light resulting from surface plasmon interactions with threefold symmetric nanostructures

B. Ashall,[1,*] B. Vohnsen,[1] M. Berndt,[1,2] and D. Zerulla[1,†]
[1]*School of Physics, University College Dublin, Belfield, Dublin 4, Ireland*
[2]*Max Planck Institute of Molecular Cell Biology and Genetics, 01307 Dresden, Germany*
(Received 30 July 2009; revised manuscript received 8 October 2009; published 9 December 2009)

The design and architecture of nanostructures for the purpose of controlling and manipulating surface plasmon polariton (SPP) dynamics is currently a focal point of research. It is driven by the predicted impact that plasmonic components will have on many future technologies. In this paper, we demonstrate the first instance of plasmon-mediated polarization reorientation observed in the far field with no associated re-emission directional change. Specifically, it is demonstrated that, as a result of the interaction between SPPs and tailor-designed nanostructures of threefold symmetry characteristics, a polarization twisting of the SPP-mediated reradiated light is attained. It is shown that the dynamics of such an interaction can be controlled externally, enabling active control of the outgoing polarization orientation. In order to further understand the origin of the processes involved, Green's function based simulations of the interactions are presented and confirm that the origin of the polarization twisting can be explained via asymmetrical in-plane SPP scattering.

DOI: 10.1103/PhysRevB.80.245413 PACS number(s): 73.20.Mf, 73.22.Lp, 71.36.+c

I. INTRODUCTION

The topic of surface plasmon polaritons (SPPs) has a research history going back just over a century[1] but in recent years has attracted renewed interest for a variety of reasons; for example, as a basis for optoelectronics[2,3] or magnetoplasmonics.[4,5] In conjunction with the forecasted applications of plasmonic components in technologies, the predominant driving force of the field is the current availability of a variety of routine nanoscale fabrication techniques that allow suitable sized structures to be made and explored as a way of harnessing SPPs (e.g., Refs. 6 and 7).

SPPs are electromagnetic (EM) surface waves confined to the interface of two materials with dielectric functions of opposite signs, i.e., metal/dielectric. They occur as a result of a resonant interaction between the illuminating wave and a collective surface electron-density oscillation of the conductor. This light/matter interaction leads to SPP modes having greater momentum than light of the same frequency. Therefore, in order to excite an SPP with light of a given frequency, the wave vector associated with the light must be adapted according to the SPP dispersion relation before excitation is possible. On the nanostructure arrayed surfaces presented here, surface periodicity coupling is the dominant excitation process while surface roughness coupling can be predominantly neglected for this examination.[8] Conversely, propagating SPP modes at a planar metal/dielectric interface are bound and guided by it, propagating until either they are liberated from the surface by some momentum-matching condition,[9] or they are lost to the metal interface through scattering processes and dissipated as heat.[10]

In a recent letter,[11] it has been demonstrated that symmetry properties of tailor-designed nanostructures have an impact on the propagation of SPPs excited on arrays of such nanostructures. It was shown that in certain orientations, 120° symmetric (rotor-shaped) nanostructures have a waveguiding effect on propagating SPPs. Highlighted in that article were the SPP excitation, propagation, and waveguiding processes on the nanostructured arrays. In particular, the primary variable explored was the *illumination polarization*. In the present paper, we will focus our examination on the interaction between the propagating plasmon and the nanostructures, and the signature of this interaction in the *outgoing polarization*, in the SPP re-emission channel. This allows us to complete the examination on the ability of the rotor nanostructures to twist the polarization of the SPP-mediated light to emit with a predictable alteration in polarization direction. We will show that the only restrictions for this polarization twisting effect are the SPP excitation conditions.

The experimental setup [Fig. 1(a)] for the far-field polarization examination is as follows: a laser source ($\lambda = 632.8$ nm) is collimated, polarized (extinction ratio of 10 000:1), and made incident on the sample which is housed on a rotation table on a fine adjust goniometer. A Fresnel Rhombus is positioned in the beamline between the polarizer and the sample. This allows for polarization angle (β) variation with uniform beam intensity, independent of any fundamental polarization of the laser. The detector (photodiode) is mounted on a computer controlled, highly resolving, angular scanner which has the sample goniometer at its fulcrum. A polarizing analyzer (rotation angle$=\gamma$) is positioned on the semispherical scanner in front of the detector. Both polarizer's (initial and analyzer) and the Fresnel Rhombus were calibrated such that their polarization axes were aligned with each other and to the optical axis of the experiment, to a combined reproducible accuracy of better than 0.25°.

The sample was prepared using standard complementary metal-oxide semiconductor fabrication processes; e-beam lithography, followed by etching to reveal the desired surface profile [Figs. 1(b) and 1(c)]. In order to facilitate SPP excitation, an 80 nm silver surface layer was subsequently deposited. For the examination presented here, we consider the interaction of the SPPs with the rotor array from four different orientations; with the excited SPP initially propagating in either the $+x$, $-x$, $+y$, or $-y$ directions. We label these orientations using compass notation (E, W, N, and S, respectively) as indicated in [Fig. 1(a)].

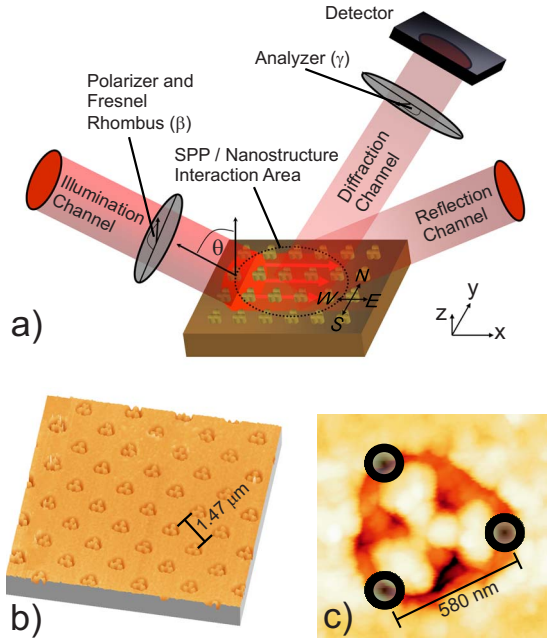

FIG. 1. (Color online) (a) Visualization of SPP excitation, propagation, and re-emission processes, on a nanostructure arrayed surface. Compass notation indicates the four examined interaction orientations; the displayed orientation in the schematic is E. (b) Atomic force microscope image of nanostructures array. (c) Individual rotor structure including indication of scattering points used in the simulations.

II. RESULTS

Locating SPP resonances is achieved using angular scans. Here, we focus on plasmon modes observable in one of the diffraction orders (the second diffraction order in the plane of incidence) where two SPP modes exist at 70° and 47°.[11] However, the observations we have made are not limited to these particular SPP modes or this specific grating order.

As previously reported,[11] it was observed that the orientation of the plasmon/rotor-structure interaction (i.e., N, S, E, or W) has a definite impact on the illumination-polarization angle (β) at which SPP related minimum reflectivities occur, as is apparent in (Fig. 2). In this plot, we see that for two orientations where the plasmon/rotor interaction is not symmetric (E and W), we observe a shift in minimum reflectivity of 30° from TM illumination polarization.

Before this illumination-polarization shift of the reflectivity minima can be confirmed to be solely a result of an interaction between propagating SPPs with the rotor structures, it must be confirmed that it is not purely a grating artifact; as it is well known that a complex grating topography can present changes in far-field intensity, independent of plasmonic effects.[12,13] Therefore, we carried out a complete angular and illumination-polarization characterization of the array for all four illumination orientations. An example of such an angular/polarization scan, for the SPP/rotor interaction in the E orientation, is presented (Fig. 3); this demonstrates that (a) the SPP excitations at illumination angles (θ) of 70° and 47° are the only pronounced intensity variations. (b) For this SPP/nanostructure orientation (E) both plasmon reflectivity

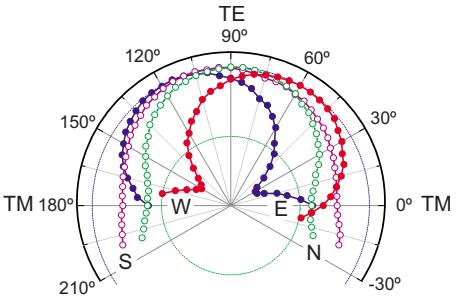

FIG. 2. (Color online) Intensity of the (+2nd) diffraction order as a function of polarization angle (β) for rotor nanostructures in the four orientations (N, S, E, and W) at the SPP excitation illumination angle (θ=70°). Intensities are individually normalized to 1. Note: the analyzer indicated in [Fig. 1(a)] is absent for the results displayed in this plot.

minima are shifted to a polarization angle (β) of TM+30°.

In order to investigate the origin and processes involved in this polarization minimum shift, we have used a polarizer/analyzer setup [Fig. 1(a)], which has previously been used to examine other SPP re-emission polarization processes.[14–16] With the illumination angle set at the strong SPP excitation angle (θ=70°), and the illumination-polarization set to TM, we have recorded the outgoing intensity monitored by the photodiode, as a function of analyzer polarization. Such an examination would typically present a $\cos^2$ function of the angle between the polarizer and the analyzer; and this is exactly what is observed for illumination angles off SPP resonance, and also for the symmetric SPP/nanostructure interaction orientations (N and S). However, for such a scan in the E and W orientations at the SPP excitation angle, we observe a deviation from a $\cos^2$ function (Fig. 4). Most notably, we observe a 5° shift in analyzer angle at which we observe a maximum. This deviation from a $\cos^2$ function indicates that the plasmon-rotor interaction is causing an additional polarizing function. More specifically, this is proof

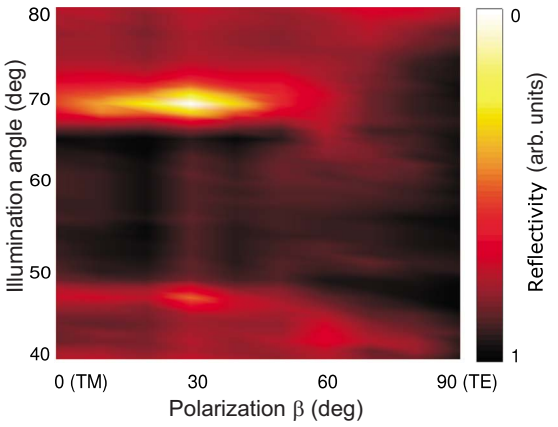

FIG. 3. (Color online) Measured reflectivity for an illumination angular range, θ=40° to 80°, and illumination polarization of TM (β=0°) to TE (β=90°). Peaks at θ=70° and 47° indicate plasmon modes. For SPP/rotor-structure interaction in the E orientation, maxima are observed for a polarization angle (β) of TM+30°. Note: the analyzer indicated in [Fig. 1(a)] is absent for the results presented in this scan.

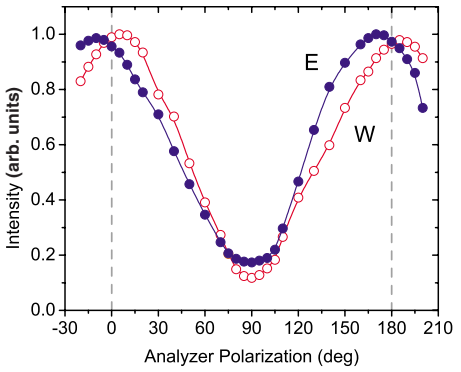

FIG. 4. (Color online) Plot of normalized intensity as a function of analyzer polarization (γ), for illumination polarization (β) of TM.

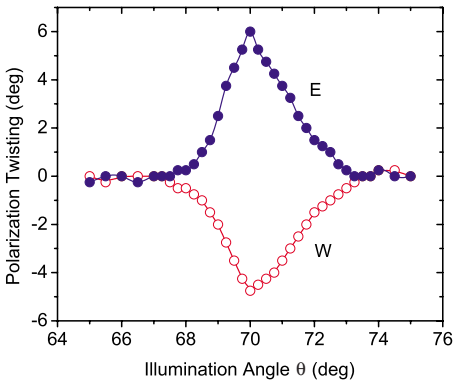

FIG. 5. (Color online) Plot of polarization twisting degree as a function of illumination angle (θ), for illumination polarization of TM.

that this interaction is twisting the polarization of the light involved in the SPP excitation and re-emission process.

Although in this setup we observe a twist of only 5°, instead of the 30° twist observed for the SPP excitation conditions in Fig. 2, both results are consistent with each other as follows: (a) for the illumination-polarization rotation experiment (Fig. 2), the minimum at TM ± 30° for E and W orientations occurs as a result of a maximum in interference between diffracted light and SPP re-emitted light at this illumination polarization. As a grating-excited plasmon is always excited with the TM component of illumination, this observation of maximum interference for illumination polarization of TM ± 30° indirectly demonstrates that the plasmon re-emitted light is also at TM ± 30°, implying that the plasmon/structure interaction has twisted the polarization and subsequently reradiated. (b) For the polarizer/analyzer experiment, the same 30° twist in polarization is now directly observed. However, in this scan the detector is subject to two light components. With an initial illumination polarization of TM, we excite a plasmon with approximately 20% efficiency, implying that the light can reach the analyzer under two separate paths: (1) in the diffraction order of interest, approximately 80% of the light is directly diffracted with no contribution to plasmon excitation. Therefore, for this component of light, no SPP/nanostructure interaction and hence, no polarization twisting takes place. Naturally, when this component of light is analyzed with a second polarizer, a $\cos^2$ function is returned, with a maximum in intensity where the illumination polarization and analyzer polarization are matching. (2) The approximate 20% of light that is involved in this particular SPP excitation will interact with the structures, and under the condition of a nonsymmetric interaction (i.e., E and W orientations) will be reradiated (neglecting SPP losses) with a twist in polarization. Specifically, for the structures examined here, this twist in polarization will be 30°. When this component of light is analyzed with a polarizer, it will also yield a $\cos^2$ function but the maximum will no longer occur for an analyzer polarization of TM but TM ± 30° instead.

In the experiment, although the light can reach the analyzer under two separate paths, these paths are indistinguishable to the detector and so the analyzer is subject to both components simultaneously. Therefore, what we experimentally measure is a function which is a combination of a 80% $\cos^2$ function with a maximum for an analyzer polarization of TM, and a 20% $\cos^2$ function with a maximum for an analyzer polarization of TM ± 30°. The outcome of this mixing of light from two separate channels is twofold: (1) the light at the detector will no longer be linearly polarized but instead (taking additional phase shifts between the two channels into account) will be elliptically polarized. (2) There is an apparent shift of approximately 5° in the polarizer analyzer experiment, as in Fig. 4.

This process is further confirmed by actively altering the distribution of light following the two paths (i.e., diffraction/SPP ratios of 80/20, 82/18,…,100/0). The variation in this ratio can be accurately controlled by tuning the illumination angle (θ). A resultant plot of observed maxima in the polarizer analyzer experiment as a function of illumination angle (Fig. 5), not only confirms the above process but also demonstrates the control of polarization twisting that can be readily achieved (steps of 0.25° twisting readily realizable).

Furthermore, the range of polarization twisting could be greatly increased by improving both structure design and surface quality, currently limiting the SPP excitation efficiency to 20%. If this excitation efficiency is increased, for example, to an achievable 50%, the far-field measurable polarization reorientation effect would be increased to 15°, and modifying the design of the structures to reorientate the plasmon more efficiently would also increase the effect.

To further understand the origin of the observed polarization twisting, numerical simulations based on elastic SPP scattering[17] have been performed. In these simulations, we examine the interaction between the SPP-associated electromagnetic field with the 120° symmetric structures, represented by several scattering points [Fig. 1(c)]. To allow us to focus solely on the origin of the polarization twisting, some simplifications of the processes contributing to the experimental observations have been deliberately made. This approach allows us to easily define and focus on the details we are interested in—namely, the plasmon **E**-field scattering—and so understand the real fundamental roots of polarization twisting process.

In the simulations (Fig. 6), an ideal planar incident SPP has been assumed, absorption losses have been neglected (as

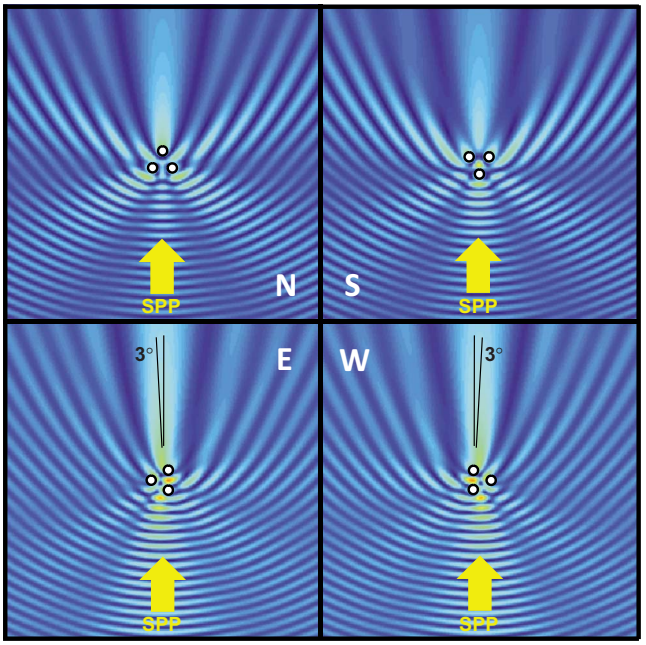

FIG. 6. (Color online) 10×10 micron field amplitude images of the incident and elastic scattered lossless SPPs. Individual rotor three-particle structures located at the corners of an equilateral triangle [as in Fig. 1(c)] produce the scattering.

these are negligible on the scale of an individual rotor structure), and for simplicity multiple SPP scattering between the structures has been omitted. Additionally, the possible local scattering and SPP excitation by individual nanostructures has been ignored. A scalar effective polarizability representative of the scattering strength of each nanostructure has been used. By implementing these simplifications, a focus can be made on the origin of the plasmon **E**-field reorientation, which ultimately determines the polarization reorientation.

Figure 6 shows results obtained with an individual rotor nanostructure oriented along the compass directions and illuminated by an incident SPP from below (propagating along the N, S, E, and W directions). The result of these simulations is that for the SPP incident in the E and W directions, a change in the main **E**-field direction of about 3° with respect to the direction of incidence is observed. This is caused by the interference of the incident SPP and the asymmetric configuration of the three-particle rotor model. It is this redirection of the plasmon **E** field that leads to the observed far-field polarization reorientation, as follows: consider a plasmon propagating in the positive x direction, at a planar metal/air interface extending in the x and y directions. If such a plasmon interacts with a surface feature that can partially scatter the plasmon in the x,y plane, part (or even all) of the plasmon will now propagate in a new direction, comprising of x and y components (e.g., as for our structures, at an angle of 30° from the original SPP propagation direction). Consider now that this plasmon can be liberated back to the far field, through the SPP momentum-matching scheme. This light will leave the sample with the following two conditions: (1) the x and y directions will be determined by the propagation direction of the plasmon while it was confined to the interface immediately prior to re-emission, i.e., the direction of the plasmons **E** field. (2) The z direction (i.e., determining the angle between the light and the interface—θ) will be determined by the momentum-matching condition according to

$$\theta = \sin^{-1}\frac{k_{\mathrm{SPP}} \mp k_{Liberation}}{k_{Light}}, \tag{1}$$

where k_{SPP} is the plasmon wave vector, k_{Light} is the wave vector of the plasmon reradiated light, and $k_{Liberation}$ is the wave vector provided by the momentum-matching scheme.

The implication of these two conditions on the polarization and free-space light propagation direction is as follows: condition (1) determines the polarization orientation and also defines the direction of the light projected in the x,y plane. Condition (2) cannot influence the polarization orientation, as a plasmon cannot have a relevant polarization component in the z orientation (for the same fundamental reason that a plasmon must be excited with TM polarization) and therefore only influences the out-of-plane angle (θ) at which the light is re-emitted.

This process has been experimentally demonstrated previously[18] for a plasmon excited in the Kretschmann configuration. In that article, instead of having a specific topographic feature to scatter the propagating SPP in a defined direction, the (near isotropic) scattering of surface roughness is used. This configuration can allow for a near uniform scattering of plasmons over a full (in plane) 360°. These scattered plasmons are free to couple back to propagating light, via evanescent coupling to optical modes at the metal/prism interface, with the out-of-plane angle (θ) determined by the SPP/light momentum-matching conditions, Eq. (1), and the angle of the light in the x,y plane determined by the propagation direction of the plasmon (i.e., its **E**-field direction) immediately prior to reradiation. This results in the well-known attenuated total reflection (ATR) ring. In Ref. 18, it was demonstrated that the polarization of the plasmon reradiated light to the ATR ring was solely determined by the **E** field of the plasmon directly before reradiation [i.e., by condition (1) above].

Applying this to a grating-excited plasmon is, in principle, the same but with the exception that the grating adds additional restrictions to the channels that reradiated light can couple to. Just as with the prism, the out-of-plane direction (θ) is determined by the free light channel that has the same momentum as the plasmon. However, unlike the prism, where a channel is available in any x,y projection, but fixed θ (i.e., the ATR ring), the grating will also restrict light to channels abiding by the diffraction equation. This condition [an extension of condition (2), above] places strict restrictions on the direction (in all planes) at which light can leave the grating, but as already justified, the polarization of the re-emitted plasmon is determined by condition (1) (i.e., the **E**-field direction of the plasmon immediately prior to the reradiating process). Indeed, it is this additional condition that enables a polarization twisting that, importantly, is *not* accompanied by a emission direction change in the light. This is typically not the case, where (as in Ref. 18 discussed above) the spatial and polarization conditions of the light are

solely defined by the plasmon **E** field prior to reradiation. In the experiment presented here, the polarization of the reradiated light is defined by the plasmon **E** field but the spatial direction of the light is defined by the grating conditions. For this reason, we can label the effect we observe as a true polarization twisting. Conversely, in the absence of a grating to determine the far-field location of the light, the polarization of the light in the plasmon re-emitted channel is not twisted, it is simply viewed in a new reference frame defined by the new direction of the light; this is comparable to the reflection of light off a tilted mirror, where the polarization of the reflected beam will be in a different plane from the incident beam but its orientation will remain constant in the reference frame of the beam itself.

Returning to the simulation results; they confirm that the **E** field and polarization reorientation is a result of an asymmetrical in-plane SPP scattering while the SPP/rotor interaction is in specific orientations (E and W). The observed reorientation of the SPP electromagnetic-field direction can be directly related to a polarization reorientation of the plasmon reradiated light. The difference in the degree of polarization twisting between the experimental observations and the simulations is accounted for in the deliberate simplifications made in the simulations. Indeed, a full finite-difference time-domain calculation would demonstrate the 30° reorientation, as observed experimentally but would present less insight into the fundamental mechanisms involved. Regardless of the simplifications of the presented simulations, their primary function here is to identify and understand the dominating mechanisms contributing to the experimentally observed polarization twisting. This has been confirmed to be as a result of an asymmetrical in-plane SPP scattering while the SPP/rotor interaction is in specific orientations (E and W).

III. CONCLUSION

Presented here is an observation of SPP-mediated polarization reorientation observed in the far field, with no associated directional change in the far-field plasmon reradiated light. We have experimentally demonstrated how tailor-designed topographic structures of threefold symmetry can be used to alter the polarization of an EM wave by a selective amount. The primary process involved in this polarization twist has been isolated and confirmed as the nonsymmetric interaction of a propagating SPP wave with the nanostructures. Specifically, the polarization orientation of the light is determined by the **E**-field orientation of the plasmon directly before its re-emission, and the far-field spatial location is determined by the grating conditions, resulting in the observed polarization twisting with no associated spatial relocation. The only apparent restrictions on the polarization rotation are found to be the initial plasmon excitation conditions. With this in mind, the possibility for optimized structures with greater polarization reorientating ability is suggested. Using Green's function based simulations, we have examined such an interaction between a propagating plasmon wave and 120° threefold symmetric structures, confirming that the origin of the far-field polarization twisting is an asymmetrical in-plane SPP scattering occurring in the near field.

ACKNOWLEDGMENTS

The authors would like to acknowledge financial support from Science Foundation Ireland (SFI) (Project Codes: ENE011, ENEF347, 07/SK/B1239a) and Enterprise Ireland (EI), and the NAP team from the Tyndall Institute in Cork, Ireland for sample preparation (Project Code SFI/NAP76).

*brian.ashall@ucd.ie
†dominic.zerulla@ucd.ie

[1] R. W. Wood, Philos. Mag. **4**, 396 (1902).
[2] S. I. Bozhevolnyi, V. S. Volkov, E. Devaux, J. Y. Laluet, and T. W. Ebbesen, Nature (London) **440**, 508 (2006).
[3] E. Ozbay, Science **311**, 189 (2006).
[4] C. Hermann, V. A. Kosobukin, G. Lampel, J. Peretti, V. I. Safarov, and P. Bertrand, Phys. Rev. B **64**, 235422 (2001).
[5] L. Sapienza and D. Zerulla, Phys. Rev. B **79**, 033407 (2009).
[6] M. Aeschlimann, M. Bauer, D. Bayer, T. Brixner, F. Javier Garcia de Abajo, W. Pfeiffer, M. Rohmer, C. Spindler, and F. Steeb, Nature (London) **446**, 301 (2007).
[7] M. Berndt, M. Rohmer, B. Ashall, C. Schneider, M. Aeschlimann, and D. Zerulla, Opt. Lett. **34**, 959 (2009).
[8] H. Raether, *Surface Plasmons on Smooth and Rough Surfaces, and on Gratings*, Tracts in Modern Physics Vol. 111 (Springer-Verlag, Berlin, 1988).
[9] B. Vohnsen and S. I. Bozhevolnyi, Appl. Opt. **40**, 6081 (2001).
[10] A. V. Zayats, I. I. Smolyaninov, and A. A. Maradudin, Phys. Rep. **408**, 131 (2005).
[11] B. Ashall, M. Berndt, and D. Zerulla, Appl. Phys. Lett. **91**, 203109 (2007).
[12] R. Petit, *Electromagnetic Theory of Gratings*, Springer Topics in Current Physics Vol. 22 (Springer, Berlin, 1980).
[13] C. H. Wilcox, *Scattering Theory for Diffraction Gratings*, Springer Applied Mathematical Sciences Vol. 46 (Springer-Verlag, Berlin, 1984).
[14] J. Malicka, I. Gryczynski, Z. Gryczynski, and J. R. Lakowicz, Anal. Chem. **75**, 6629 (2003).
[15] I. Gryczynski, J. Malicka, Z. Gryczynski, and J. R. Lakowicz, Anal. Biochem. **324**, 170 (2004).
[16] G. Isfort, K. Schierbaum, and D. Zerulla, Phys. Rev. B **73**, 033408 (2006).
[17] S. I. Bozhevolnyi and V. Coello, Phys. Rev. B **58**, 10899 (1998).
[18] G. Isfort, K. Schierbaum, and D. Zerulla, Phys. Rev. B **74**, 033404 (2006).